

Research Article

Intestinal Lymphatic Delivery of Praziquantel by Solid Lipid Nanoparticles: Formulation Design, *In Vitro* and *In Vivo* Studies

Amit Mishra, Parameswara Rao Vuddanda, and Sanjay Singh

Department of Pharmaceutics, Indian Institute of Technology, (Banaras Hindu University), Varanasi 221 005, India

Correspondence should be addressed to Sanjay Singh; ssingh.phe@iitbhu.ac.in

Received 29 July 2013; Accepted 5 November 2013; Published 19 February 2014

Academic Editor: John A. Capobianco

Copyright © 2014 Amit Mishra et al. This is an open access article distributed under the Creative Commons Attribution License, which permits unrestricted use, distribution, and reproduction in any medium, provided the original work is properly cited.

The aim of the present work was to design and develop Praziquantel (PZQ) loaded solid lipid nanoparticles (PZQ-SLN) to improve the oral bioavailability by targeting intestinal lymphatic system. PZQ is practically insoluble in water and exhibits extensive hepatic first-pass metabolism. PZQ SLN were composed of triglycerides, lecithin and various aqueous surfactants; were optimized using hot homogenization followed by ultrasonication method. The optimized SLN had particle size of 123 ± 3.41 nm, EE of $86.6 \pm 5.72\%$. The drug release of PZQ-SLN showed initial burst release followed by the sustained release. In spite of zeta potential being around -10 mV, the optimized SLN were stable at storage conditions ($5 \pm 3^\circ\text{C}$ and $25 \pm 2^\circ\text{C}/60 \pm 5\%$ RH) for six months. TEM study confirmed the almost spherical shape similar to the control formulations. Solid state characterization using differential scanning calorimeter (DSC) and powder X-ray diffraction (PXRD) analysis confirmed the homogeneous distribution of PZQ within the lipid matrix. The 5.81-fold increase in $\text{AUC}_{0 \rightarrow \infty}$, after intraduodenal administration of PZQ-SLN in rats treated with saline in comparison to rats treated with cycloheximide (a blocker of intestinal lymphatic pathway), confirmed its intestinal lymphatic delivery. The experimental results indicate that SLN may offer a promising strategy for improving the therapeutic efficacy and reducing the dose.

1. Introduction

Praziquantel (PZQ) is a pyrazinoisoquinoline drug used in both veterinary and human medicine as the drug of choice against many parasitic diseases caused by cestodes and trematodes. It is widely used in developing countries for the treatment of schistosomiasis [1] and neurocysticercosis [2]. Moreover, PZQ has become the cornerstone for Hydatid control campaigns worldwide [3]. For its efficacy, safety, and comparative cost effectiveness, PZQ is included in the World Health Organization model list of essential drugs [4]. PZQ exhibits poor oral bioavailability because of its low aqueous solubility, extensive hepatic first-pass metabolism, and the short plasma half-life (0.8–1.5 hours) [5–7]. Although PZQ is a very effective anthelmintic, the above-mentioned shortcomings necessitate frequent administration of high oral doses of PZQ to overcome first-pass metabolism and to achieve sufficient plasma concentrations of PZQ at the larval tissues for eradication of cestode infection [8].

In previous studies, researchers have focused either to increase PZQ concentrations in plasma by concomitant administration of cimetidine or food [9, 10] or to improve the dissolution rate using adjuvants such as cyclodextrins and polyvinylpyrrolidone [11, 12]. Liposomes have also been attempted to improve bioavailability [13] as well as the antischistosomal activity of PZQ [14]. The development of resistance in certain countries to PZQ also calls for developing novel drug delivery systems [6, 15]. Strategies currently being investigated to overcome these shortcomings are the improvement of oral bioavailability using solid lipid nanoparticles (SLN) and to assess alternative route for drug administration using SLN [16, 17].

Intestinal lymphatic delivery is an emerging option for site-specific oral absorption of peptides, proteins, drugs, and vaccines [18, 19]. This avoids first-pass metabolism following peroral administration. Gastrointestinal tract is richly supplied with blood and lymphatic vessels. Since rate of fluid flow in portal blood is about 500-fold higher than that in intestinal

lymph, the majority of the dietary compounds are transported to portal blood [20, 21]. Highly lipophilic compounds such as long-chain triglycerides with chain lengths of 14 and above would reach systemic circulation via the intestinal lymphatics [22, 23]. Several mechanisms for delivering drugs to or through lymphatics following the peroral drug delivery include paracellular mechanism, transport through M cells of Peyer's patches, and transcellular mechanism [19–22]. Among them, transcellular absorption is the most promising mechanism for the absorption of lipid carriers. The strategies such as prodrug synthesis, permeation enhancers, liposomes, microemulsions, polymeric nanoparticles, self-emulsifying drug delivery systems (SEDDS), and solid lipid nanoparticles (SLN) have been explored for the delivery of bioactives to intestinal lymphatics [19, 23, 24].

SLN represents an alternative to traditional colloidal carriers (emulsions, liposomes, and polymeric nanoparticles) in enhancing the oral bioavailability of poorly soluble drugs. These particulate systems contain solid lipids (remain in the solid state at room and body temperatures) as matrix material which possesses adhesive properties that make them adhere to the gut wall and release the drug exactly where it should be absorbed [25]. They offer the advantages over traditional colloidal systems such as enhanced physical stability, protection of drug degradation in the body, possibility of controlled drug release, low or total absence of toxicity; drug targeting, and different possible administration routes [26]. Moreover, the lipid core of SLN may mimic chylomicron formation by enterocytes, which dissolve and assimilate lipophilic drug molecules and promote the absorption of water-insoluble drugs into intestinal lymphatics by the transcellular mechanism of lipid absorption [22]. The use of SLN as carrier for bioactives through lymphatic regions following oral administration has been investigated and documented by many researchers [19, 24, 27].

In the present study, PZQ loaded SLN were designed and developed to improve the oral bioavailability by targeting intestinal lymphatic system. SLN were prepared by hot homogenization followed by ultrasonication method. The effects of various process and formulation parameters such as homogenization time, ultrasonication time, and surfactant/lipid composition on the physicochemical properties of SLN were investigated. The stability was assessed over a period of six months. The pharmacokinetic behavior of SLN was assessed in rats to validate the effectiveness of SLN in enhancing the oral bioavailability of PZQ. The intestinal transport of SLN after intraduodenal administration was also investigated to clarify its lymphatic delivery.

2. Materials and Methods

2.1. Materials. Praziquantel (PZQ) was a kind gift from Wockhardt Research Centre (Aurangabad, India). Tripalmitin (TP) and tristearin (TS) were purchased from SRL (Mumbai, India), while poloxamer 188 (P188) and poloxamer 407 (P407) were kindly supplied by BASF (India). Trimyristin and lecithin granular (LG) were purchased from Sigma-Aldrich (Lyon, France) and Acros Organics (New Jersey,

USA), respectively. Tween 80 (Tw80) and dialysis membrane (molecular weight cutoff—MWCO between 12,000 and 14,000 daltons) were purchased from HiMedia (Mumbai, India). Nanosep Centrifugal filter devices (Omega Membrane, MWCO 100 kD) were purchased from Pall Life Sciences (Mumbai, India). HPLC grade acetonitrile and methanol were obtained from SRL (Mumbai, India). The water used in all experiments was ultrapure, obtained from a Millipore-DirectQ UV ultrapure water system (Millipore, France). All other chemicals and reagents were of analytical grade.

2.2. Partitioning Behavior of the Drug between Lipids and Water. PZQ (20 mg) was dispersed in a mixture of melted triglyceride (2 g) and hot water (2 mL). The mixture was kept on a hot water bath shaker maintained at temperature 10°C above the melting point of concerned lipids and shaken for 30 min. Aqueous phase was then separated after cooling by centrifugation with the help of Nanosep centrifuge tubes and analyzed for PZQ content by HPLC [28, 29].

2.3. Preparation of PZQ-Loaded SLN. PZQ-loaded SLN were prepared by hot homogenization followed by ultrasonication method [28]. Briefly, the lipid phase consisting of PZQ (0.05–0.2% w/v); lipid (1–10% w/v) and lipophilic surfactant (lecithin granular, 0.5–2.5% w/v) were weighed precisely with an electronic balance (Shimadzu AX100, Japan) and dissolved in a mixture of chloroform and methanol (2 : 1). The mixture was transferred to rota-evaporator at 300 mbar, 50°C (IKA RV 10 digital, Germany), to obtain a thin lipid layer. Nitrogen was blown on the lipid layer to remove traces of organic solvents, if any. The hot aqueous phase containing hydrophilic surfactant (1–3% w/v) heated to same temperature of the molten lipid phase was added to thin lipid layer and hydrated for 30 min. A coarse hot o/w emulsion thus obtained was homogenized at 13,000 rpm with the help of Ultra-turrax (T 25 digital, IKA, Germany) for 2.5–10 min. The obtained pre-emulsion was sonicated with probe ultrasonicator (UP 200 H, Hielscher Ultrasonics GmbH, Germany, 13 mm microprobe with amplitude 55% at 200 W) for 2.5–10 min. To prevent recrystallization during homogenization and ultrasonication, production temperature was kept at least 5°C above the melting point of lipid. The hot nanoemulsion (o/w) obtained was quickly poured into 200 mL cold water to obtain PZQ incorporated SLN. The SLN were collected by centrifugation at 15,000 g (Cooling Centrifuge BL 24; Remi Instruments Ltd., India) for 90 min at 4°C and washed three times with purified water. The SLN were suspended in purified water and prefrozen under –40°C in deep freezer for 12 hr. The samples were lyophilized for 48 h (Lypholizer, Decibel, India) under vacuum at a temperature of –40°C using mannitol (5% w/v) as a lyoprotectant to obtain SLN powders and stored at 4°C. The control SLN was prepared in the same way without adding the PZQ.

2.4. Formulation Design. The processing parameters such as homogenization time (HT), ultrasonication time (ST), and total volume of formulation (VF) were optimized as described previously [30]. The following formulation parameters were kept constant: lipophilic surfactant (LG)

concentration (LSC) = 2% w/v, hydrophilic surfactant (PI88) concentration (HSC) = 2% w/v, and Lipid (TP) concentration (LC) = 5% w/v, drug concentration (DC) = 0% w/v.

The scheme for optimization is mentioned below:

- homogenization time (HT): 2.5, 5, 10, and 15 min, while ST = 10 min, and VF = 50 mL;
- sonication time (ST): 2.5, 10, and 15 min, while HT = 5 min, and VF = 50 mL;
- volume of formulation (VF): 50, 100, and 200 mL, while HT = 5 min, and ST = 10 min.

The formulation parameters such as lipid type and concentration, surfactant type and concentration, and drug concentrations for preparing SLN were also optimized using formulation design (Table 2) as described previously [31], after determination of optimum process parameters (i.e., HT = 5 min, ST = 10 min, and VF = 50 mL).

2.5. Determination of Particle Size, Polydispersity Index, and Zeta Potential. The mean particle size (PS), polydispersity index (PI), and zeta potential (ZP) were measured by photon correlation spectroscopy (PCS) using a Particle Analyzer (Delsa Nano C; Backman Coulter, USA) at 25°C.

2.6. Transmission Electron Microscopy (TEM) Studies. Lyophilized SLN were dispersed directly in ultrapure water. A drop of SLN dispersion was spread onto a 200-mesh copper grid coated with carbon film and stained with 2% w/v phosphotungstic acid. The grid was dried at room temperature and observed by the TEM (TECNAI-20 G², FEI, Holland).

2.7. Drug Loading and Entrapment Efficiency. PZQ-SLN (100 µL) was diluted to 10 mL with chloroform/methanol mixture (2:1) and vortexed to extract drug from lipid. The obtained solution was filtered through 0.45 µm PVDF membrane filter and total weight of drug in system (A_t) was determined by HPLC. The entrapment efficiency (EE) of the PZQ-SLN was determined indirectly by calculating the amount of free PZQ (unentrapped) in the aqueous phase of the SLN dispersion. After a suitable dilution, PZQ-SLN (500 µL) was transferred to the upper chamber of Nanosep centrifuge tubes and centrifuged (5000 rpm for 30 minutes). The SLN along with encapsulated drug were retained in the upper chamber, while the unentrapped PZQ along with dispersion medium moved through the filter membrane into the lower chamber of Nanosep. The amount of unentrapped PZQ (A_{un}) in the aqueous phase after isolation of the system was detected by HPLC. The entrapment efficiency (EE) and drug loading (DL) of SLN were calculated by equations (1) and (2), respectively [31–33],

$$EE (\%) = \left[\frac{(A_t - A_{un})}{A_t} \right] \times 100, \quad (1)$$

$$DL (\%) = \left[\frac{(A_t - A_{un})}{(A_t - A_{un} + A_l)} \right] \times 100, \quad (2)$$

where A_t , A_{un} , and A_l were the weight of total drug in the system, analyzed weight of unentrapped drug, and weight of lipid added in the system, respectively.

Praziquantel was quantified by a validated HPLC method [29] using an HPLC system (Waters 2998 system, Waters, USA) equipped with a PDA detector set at 217 nm and C18 column (Spherisorb ODS2, 250 mm × 4.60 mm i.d.; 5 µm, Waters, USA). The mobile phase, a mixture of acetonitrile/water at ratio of 70/30, was kept at flow rate of 1.0 mL/min at ambient temperature. Aliquots of 20 µL clear supernatant samples were injected into the HPLC system.

2.8. Accelerated Stability Studies. The lyophilized powder sample of optimized formulation was subjected to accelerated stability studies according to International Conference on Harmonisation (ICH) Q1A (R2) guidelines [30, 33]. PZQ-SLN formulations under a sealed condition were kept at refrigerated temperature (5 ± 3°C) and in stability chamber maintained at 25 ± 2°C/60 ± 5% RH and pH conditions (SGF pH 1.2 for 2 hours, SIF pH 7.5 for 6 hours). The samples were analyzed periodically for any change in average particle size and drug content for a total period of six months.

2.9. Differential Scanning Calorimetry (DSC) Studies. Thermograms of the different samples were obtained using a DSC (DSC 30; Mettler-Toledo, Viroflay, France). The instrument was calibrated with indium (calibration standard, purity >99.999%) for melting point and heat of fusion. A heating rate of 10°C/min was employed in the temperature ranges between 20 and 200°C, under a nitrogen purge (80 mL/min).

2.10. X-Ray Diffractometry (XRD) Studies. Powder X-ray diffraction (PXRD) studies were performed by powder X-ray diffractometer (Siemen's D-5000, Germany) using Cu-Kα radiation (40 kV, 30 mA). The samples were scanned over a 2θ range of 5° to 50° at a step size of 0.045° and step time of 0.5 s.

2.11. In Vitro Drug Release Studies. *In vitro* release studies were performed using dialysis bag diffusion technique [18, 32]. The dialysis membrane was soaked in dissolution medium for 12 hours prior usage. The SLN dispersion (equivalent to 2 mg of PZQ) was placed in the dialysis bag; both ends were tightly sealed and immersed into the dialysis medium (75 mL, 0.1 M HCl for two hours and phosphate buffer pH 6.8 for 24 hours) kept at 37°C ± 1°C and stirred magnetically at 100 rpm. At regular time intervals, aliquots of dialysate samples were withdrawn and an equal volume of dissolution medium was replaced by fresh medium, so as to maintain a constant volume throughout the study. The aliquots were filtered with a 0.1 µm filter and were analyzed for PZQ concentration by HPLC (see Section 2.7). Praziquantel aqueous dispersion in 0.5% methyl cellulose was used as control.

2.12. In Vivo Study

2.12.1. Animal Study Protocol. The animal experiment protocol was approved by the Animal Ethical Committee of the Institute of Medical Sciences, Banaras Hindu University,

Varanasi, India. Charle Foster strain albino rats (250 ± 20 g) of either sexes were housed and handled according to institutional guidelines. All animals were starved overnight prior use and divided into two groups comprising six animals in each group ($n = 6$).

2.12.2. Pharmacokinetic Study. The *in vivo* performance of SLN was evaluated via oral administration of the PZQ formulations at a dose of 50 mg/kg. All animals of group I (control group) were given an oral dose of PZQ suspension (0.5% w/v methyl cellulose suspension of pure drug); group II (treated group) was administered orally with an equivalent dose of TP-SLN (F25). The formulations were administered orally with the aid of a syringe and infant feeding tube. Blood samples (0.3–0.5 mL) were drawn by retroorbital venous plexus puncture with the aid of glass capillary tubes in heparinized Eppendorf tubes at 0.08, 0.17, 0.33, 0.5, 1, 2, 4, 6, 8, 12, 18, 24, 30, 36, and 48 hrs post oral dose. Each blood sample was centrifuged at 12,000 g for 10 min; the plasma obtained was stored at -20°C until analysis by HPLC.

2.12.3. Quantification of Plasma Concentration by HPLC. Samples were analyzed by an HPLC method previously reported with little modification [29]. Briefly, 200 ng internal standard working solution (diazepam 20 $\mu\text{g}/\text{mL}$) was added to 200 μL plasma. The samples were mixed in a vortex for 4–5 s, and then 200 μL mixture of methyl alcohol and acetonitrile (1:1, v/v) was added. The mixture was vortexed for 3.0 min to allow complete mixing, followed by centrifugation at 15,000 g (Cooling Centrifuge, Remi, India) for 30 min. The 20 μL of supernatant was injected onto the HPLC column. The HPLC system (Waters, USA) with PDA detector was used which consisted of binary pumps (Waters 515) and PDA detector (Waters 2998). The separation was carried out on a reversed phase C18 column (Spherisorb ODS2 5 μm , 250×4.6 mm, Waters, USA) using acetonitrile-water (70:30) as mobile phase running at a flow rate of 1.0 mL/min at 217 nm. The chromatographic analysis was carried out at room temperature. The data was processed by means of Ezchrome Elite software (Waters, USA).

2.12.4. Pharmacokinetic Analysis. Pharmacokinetic analysis was performed on each individual set of data, using the pharmacokinetic software Winnonlin 5.3 (Pharsight, CA) using a noncompartmental method.

2.13. Assessment of Intestinal Lymphatic Transport. The intestinal lymphatic transport of PZQ-SLN was evaluated via intraduodenal administration of the PZQ-SLN formulation at a dose of 50 mg/kg. All the rats were starved overnight prior use and divided into two groups comprising six animals in each group ($n = 6$). The animals of group I (treated group) were given cycloheximide (CHM) solution (0.6 mg/mL) at a dose of 3 mg/kg intraperitoneally (i.p.); group II (control group) was given equal volume of saline intraperitoneally (i.p.). CHM is known to inhibit the secretion of chylomicrons from the enterocytes [33–35]. At one hour after injection, rats were anesthetized with 60 mg/kg of thiopentone sodium

[28]. Small incision was made at abdomen and duodenum was located. PZQ-SLN (F25) was administered directly into the duodenum with syringe. The duodenum was ligated just under the pylorus and skin of the main incision was sutured carefully [28]. Blood samples were collected and processed as described in oral route.

2.14. Statistical Analysis. The results were expressed as mean \pm standard deviation (SD). Statistical comparisons of the experimental results were performed by Student's *t*-test and one way analysis of variance (followed by post-Tukey's multiple comparison test). In all cases, *P* value less than 0.05 was considered to be significant.

3. Results and Discussion

3.1. Partitioning Behaviour of PZQ in Lipid Matrix. Solubility of drug in lipid is one of the most important factors for determining drug loading capacity of the SLN [36]. Partitioning behaviour of praziquantel (PZQ) was tested in three triglycerides with different chain lengths, trimyristin (C_{14}), tripalmitin (C_{16}), and tristearin (C_{18}). Partition coefficients (ratio of the amount of PZQ in lipid to the amount of PZQ in aqueous phase) obtained were 18.3 ± 2.32 , 39.4 ± 4.87 , and 36.3 ± 4.22 for TM, TP, and TS, respectively. Among them, tripalmitin showed the highest solubilization capacity followed by tristearin and trimyristin. The solubilizing capacity of TP and TS was comparatively similar and, thus, TP and TS were chosen as lipid matrix for further studies.

3.2. Fabrication of Praziquantel Nanoparticles. In the present study, a simple, economical, and reproducible method, that is, modified hot homogenization followed by ultrasonication (at above the melting point of the lipid), was employed for the preparation of PZQ-SLN. Solvent system chloroform/methanol (2:1) was used to disperse the praziquantel homogeneously in the lipid. Coevaporation of the lipid and drug from organic solvents in a round bottom flask was found to produce practically the highest drug entrapment in liposomes and SLN [13, 28].

3.3. Effect of Process Variables. The process parameters such as homogenization time (HT), ultrasonication time (ST), and the total volume of formulation (VF) have a significant effect on the physicochemical properties of the SLN produced by hot homogenization followed by ultrasonication method [30, 31]. Effect of different process variables on PS, PI, and ZP was observed and presented in Table 1. The process parameters were optimized for preparing SLN with a small particle size (<200 nm) together with a low polydispersity (<0.3).

3.3.1. Effect of Homogenization Time. As shown in Table 1, PS and PI were not affected by increasing homogenization time (HT). The homogenization step is considered to be an intermediate step and responsible mainly for primary emulsification of lipid in aqueous phase [28, 31]. ZP was around -10 mV because of the presence of steric stabilizer.

TABLE 1: Effect of different process parameters on particle size (PS), polydispersity index (PI), and zeta potential (ZP).

Process variables	PS (nm)	PI	ZP (-mV)
Homogenization time (HT)			
2.5 min	146.7 ± 2.59	0.463 ± 0.027	10.1 ± 0.29
5 min	132.3 ± 1.43	0.289 ± 0.024	9.8 ± 0.38
10 min	121.6 ± 1.58	0.213 ± 0.012	9.9 ± 0.45
15 min	129.2 ± 1.72	0.392 ± 0.019	9.8 ± 0.52
Sonication time (ST)			
2.5 min	421.1 ± 7.69	0.631 ± 0.034	9.7 ± 0.49
5 min	218.7 ± 7.14	0.512 ± 0.031	9.6 ± 0.42
10 min	133.4 ± 1.73	0.404 ± 0.039	9.7 ± 0.38
15 min	130.3 ± 1.82	0.293 ± 0.044	9.7 ± 0.47
Volume of formulation (VF)			
50 mL	127.4 ± 1.75	0.289 ± 0.037	9.6 ± 0.42
100 mL	132.4 ± 1.32	0.314 ± 0.038	9.7 ± 0.38
200 mL	134.2 ± 1.58	0.396 ± 0.042	9.7 ± 0.47

TABLE 2: Formulation composition and the effect of different formulation variables on particle size (PS), polydispersity index (PI), zeta potential (ZP), entrapment efficiency (EE), and drug loading (DL).

Code	Lipid	Surfactant	LSC (%w/v)	HSC (%w/v)	LC (%w/v)	DC (%w/v)	PS (nm)	PI	ZP (-mV)	EE (%)	DL (%)
F1	TP	P188	0.5	2.0	5.0	0.1	279.8 ± 29.7	0.441 ± 0.038	08.2 ± 0.59	62.7 ± 0.59	1.24 ± 0.04
F2	TP	P188	1.0	2.0	5.0	0.1	167.4 ± 15.8	0.397 ± 0.042	10.9 ± 0.46	68.9 ± 1.21	1.36 ± 0.02
F3	TP	P188	1.5	2.0	5.0	0.1	118.4 ± 12.3	0.283 ± 0.039	15.8 ± 0.57	75.6 ± 1.32	1.49 ± 0.03
F4	TP	P188	2.0	2.0	5.0	0.1	116.9 ± 12.8	0.267 ± 0.041	18.2 ± 0.43	79.5 ± 0.93	1.57 ± 0.04
F5	TP	P188	2.5	2.0	5.0	0.1	129.9 ± 12.8	0.289 ± 0.041	20.7 ± 0.43	84.7 ± 0.78	1.67 ± 0.05
F6	TP	P188	1.5	1.0	5.0	0.1	321.2 ± 11.4	0.382 ± 0.058	19.8 ± 0.68	63.2 ± 0.83	1.25 ± 0.04
F7	TP	P188	1.5	1.5	5.0	0.1	297.5 ± 23.3	0.241 ± 0.027	17.3 ± 0.73	68.5 ± 0.69	1.35 ± 0.03
F8	TP	P188	1.5	2.0	5.0	0.1	164.8 ± 3.92	0.294 ± 0.032	15.7 ± 0.47	78.9 ± 0.74	1.55 ± 0.05
F9	TP	P188	1.5	2.5	5.0	0.1	117.3 ± 0.93	0.248 ± 0.043	12.6 ± 0.65	82.4 ± 0.65	1.62 ± 0.06
F10	TP	P188	1.5	3.0	5.0	0.1	098.6 ± 0.98	0.236 ± 0.029	09.7 ± 0.57	80.6 ± 0.58	1.59 ± 0.04
F11	TP	P188	1.5	2.0	1.0	0.1	59.2 ± 2.73	0.334 ± 0.038	11.3 ± 0.63	47.2 ± 0.75	4.51 ± 0.07
F12	TP	P188	1.5	2.0	2.5	0.1	93.2 ± 2.16	0.289 ± 0.041	12.5 ± 0.84	64.8 ± 0.87	2.53 ± 0.05
F13	TP	P188	1.5	2.0	5.0	0.1	122.4 ± 0.92	0.342 ± 0.049	10.6 ± 0.59	80.4 ± 0.67	1.58 ± 0.04
F14	TP	P188	1.5	2.0	5.0	0	110.2 ± 1.89	0.211 ± 0.039	9.8 ± 0.73	—	—
F15	TP	P188	1.5	2.0	5.0	0.025	123.9 ± 1.73	0.276 ± 0.047	9.9 ± 0.69	98.2 ± 0.56	0.49 ± 0.02
F16	TP	P188	1.5	2.0	5.0	0.05	129.3 ± 2.98	0.292 ± 0.057	9.9 ± 0.75	92.1 ± 0.63	0.91 ± 0.03
F17	TP	P188	1.5	2.0	5.0	0.1	198.3 ± 9.18	0.316 ± 0.062	10.8 ± 0.56	81.7 ± 0.57	1.61 ± 0.04
F18	TP	P188	1.5	2.0	5.0	0.2	241.4 ± 11.43	0.357 ± 0.059	11.9 ± 0.65	69.3 ± 0.79	2.70 ± 0.05
F19	TP	P188	1.5	2.0	5.0	0.1	132.3 ± 2.93	0.248 ± 0.043	11.6 ± 0.6	78.4 ± 0.65	1.54 ± 0.04
F20	TS	P188	1.5	2.0	5.0	0.1	169.3 ± 4.19	0.317 ± 0.037	9.8 ± 0.58	78.4 ± 0.14	1.54 ± 0.04
F21	TM	P188	1.5	2.0	5.0	0.1	132.2 ± 2.43	0.252 ± 0.041	9.7 ± 0.79	75.5 ± 0.44	1.43 ± 0.04
F22	TP	Tw80	1.5	2.0	5.0	0.1	313.4 ± 21.43	0.382 ± 0.058	9.8 ± 0.73	72.6 ± 0.93	1.25 ± 0.03
F23	TP	P407	1.5	2.0	5.0	0.1	121.2 ± 11.4	0.218 ± 0.058	9.6 ± 0.68	73.2 ± 0.73	1.37 ± 0.04
F24	TP	P188	1.5	2.0	5.0	0.1	132.3 ± 2.93	0.248 ± 0.043	11.6 ± 0.65	78.4 ± 0.65	1.54 ± 0.04
F25	TP	P188	2.0	2.5	5.0	0.05	123.1 ± 3.41	0.219 ± 0.052	11.2 ± 0.46	86.6 ± 0.94	1.70 ± 0.05
F26	TS	P188	2.0	2.5	5.0	0.05	132.6 ± 4.29	0.263 ± 0.073	10.9 ± 0.62	84.3 ± 0.81	1.66 ± 0.05

Homogenization time of 5 min was sufficient to obtain SLN with suitable PS and PI.

3.3.2. Effect of Sonication Time. Ultrasonication time (ST) plays a major role in obtaining a formulation with narrow particle size distribution. Sonication breaks the coarse emulsion drops to nanodroplets and is responsible for final particle size of SLN [30, 31]. Increased ST significantly decreased both PS and PI (Table 1). The sonication time of 10 min was considered suitable for SLN production. ZP was found to be around -9.7 mV.

3.3.3. Effect of Volume of Formulation. In case of high shear homogenization, the basic mechanism is the homogenizer mixing efficiency, which is mainly affected by the volume of the dispersion [37]. A total volume of 50 mL corresponded to the best results in terms of PS and PI of the SLN (Table 1).

3.4. Effect of Formulation Variables. A variety of surfactants have been used for the preparation of SLN including phospholipids, bile salts, poloxamers, and other ionic/nonionic surfactants. The stabilization of SLN with phospholipids and an additional surfactant rather than with a single surfactant frequently yields SLN with a more homogeneous appearance and lower tendency to form macroscopic particles [38]. In the present study, a phospholipid (lecithin) along with a nonionic surfactant was used to stabilize the nanoparticles. The lecithin granular was selected as lipophilic surfactant as the schistosomiasis parasite has a high affinity for phospholipids and it is reported that ingested lipids are found to be incorporated into stable parasite structures rather than utilized by the host for degradative energy-yielding metabolism [39].

3.4.1. Effect of Lipophilic Surfactant Concentration. The lipophilic surfactant used in present study was lecithin granular (LG) which in combination with hydrophilic surfactant (P188) could effectively cover the SLN and, thus, prevent agglomeration. The PS measurements of SLN revealed that the incorporation of lecithin up to 2.0% w/v (F1 to F4) led to a concentration-dependent particle size reduction down to 117 nm. Further, increase of lecithin up to 2.5% w/v (F5) caused no further decrease in PS (Table 2). This observation is related to the increased concentration of surfactant (lecithin) in formulations, which reduces surface tension and facilitates the droplet division during homogenization [40]. A critical LG concentration was reached at 2.0% w/v, addition of LG above this concentration did not cause a further decrease in particle size, and no additional surface area was provided to accommodate lecithin [41]. The combination of P188 and LG as surfactant showed a significant effect on zeta potential. SLN prepared with higher LG concentration as a zwitterionic surfactant possessed the highest zeta potential of -20.7 mV (F5). EE was increased from 62% w/w (F1) to 84.7% w/w (F5) as the LG content was increased from 0.5% to 2.5% w/v; this may be due to increase in lipid content as lecithin is a phospholipid (Table 2).

3.4.2. Effect of Hydrophilic Surfactant Concentration. Different hydrophilic surfactant (P188) concentrations enabled not only the control of the particle size, but in addition also allowed the formation of surface charge modified particles. PS and PI decreased with increasing P188 concentration up to 2.5% w/v (Table 2). These observations might be due to production and stabilization of smaller lipid droplets at higher HSC as enough amount of surfactant was present to stabilize the SLN. EE also increased with increasing HSC. This could be due to the presence of sufficient HSC which helped the drug to remain within the lipid particles and/or on the surface of the particles [42]. ZP decreased as the concentration of P188 increased. This could be attributed to the increased amounts of nonionic surfactant which counteract the negative charge of the particle surface, which is believed to go along with a displacement of the plane of shear of the nanoparticles and a steric stabilization of the stern layer.

3.4.3. Effect of Lipid Concentration. The amount of lipid which solubilizes the drug in formulation has significant effect on the particle size of the SLN. The increase in lipid concentration (LC) from 1.0 to 5.0% w/v (F11 to F13) resulted in a significant increase in PS of the SLN (Table 2). The higher viscosity of the dispersed phase due to the high lipid content would negatively affect the homogenizer efficiency and distribution of sonication energy [37]. At higher LC, the amount of surfactant available may not be sufficient to cover newer particle surfaces resulting in larger particles and more heterogeneous particle size distribution. The EE increased with increasing LC. This may be explained on the fact that, as there was increase in the lipid phase, more amount of the lipid was available for the PZQ to dissolve.

3.4.4. Effect of Drug Concentration. The PS and PI of the SLN significantly increased with increasing drug concentration (0.025–0.2% w/v). ZPs were around -10 mV in all cases, whereas EE significantly decreased with increasing DC (F14 to F18). This could be due to increase in drug to lipid ratio with increasing DC at fixed amount of lipid, which resulted in higher free drug and lower EE.

3.4.5. Effect of Lipid Type. The lipid core material was found to affect the extent of PZQ loading in SLN. As observed with TP-SLN (F19) and TS-SLN (F20), the EE was estimated to be $79.3 \pm 0.22\%$ and $78.4 \pm 0.14\%$, respectively (Table 2). However, the PS was found to be relatively lower in case of TP in comparison to TS.

3.4.6. Effect of Surfactant Type. Poloxamer series of surfactant (poloxamer 188 and poloxamer 407) produced particles of lower PS and higher EE in comparison to Tween 80 (Table 2). The inclusion of P188 as hydrophilic surfactant produced SLN with a particle size of about 132.3 ± 2.93 nm and a PI of about 0.248 ± 0.043 . EE was slightly higher when P188 was used than P407. The results indicate that steric stabilizer (P188) in combination with zwitterionic lipophilic surfactant (LG) can be suitable for the production of desired SLN.

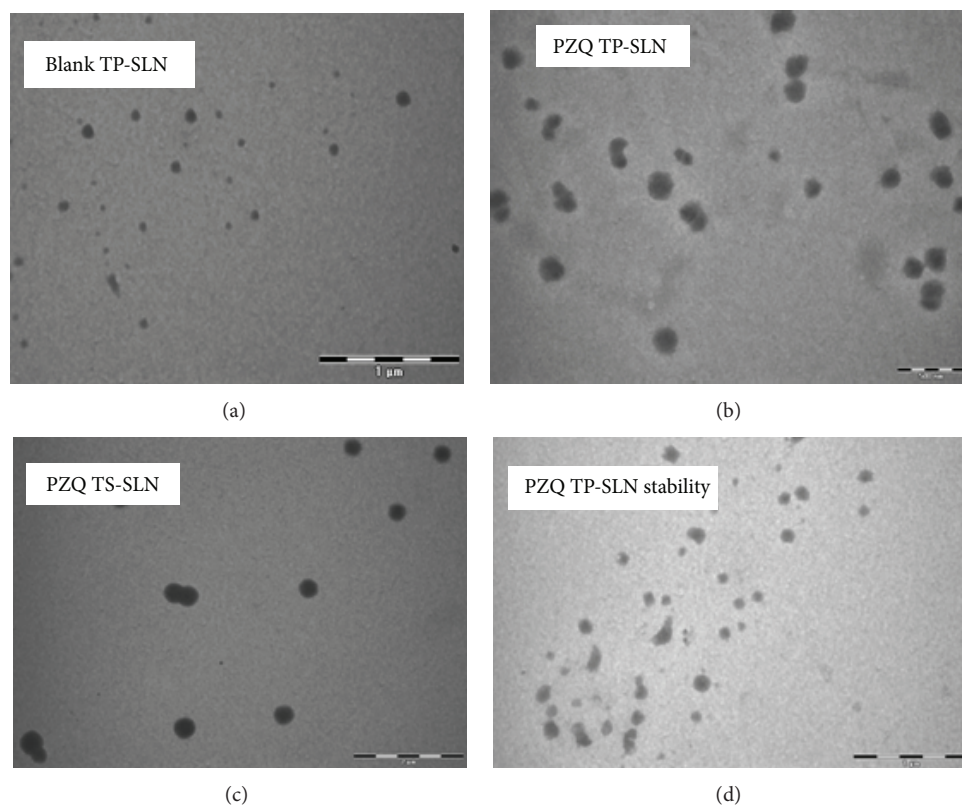


FIGURE 1: Transmission electron micrographs of different solid lipid nanoparticles. (a) Blank PZQ SLN, (b) PZQ TP-SLN, (c) PZQ TS-SLN, and (d) PZQ TP SLN stored at refrigerated temperatures for six months.

From the results obtained, the optimized formulation conditions were decided as follows: LSC = 2% w/v, HSC = 2.5% w/v, LC = 5% w/v, DC = 0.05% w/v, lipid = TP, lipophilic surfactant = LG, and hydrophilic surfactant = P 188.

3.5. Shape and Morphology. The TEM images of blank SLN, PZQ TP-SLN, PZQ TS-SLN, and PZQ TP-SLN stability sample (six months at refrigerated conditions) are shown in Figures 1(a)–1(d). The TEM revealed that particles were almost spherical with smooth surface morphology. The blank SLN and the PZQ-loaded SLN being similar in appearance reflects that encapsulation of PZQ did not affect the morphology of SLN. Moreover, despite the some nanoparticles aggregation after storage (Figure 1(d)), SLN formulations with colloidal sizes were still observed. These results are in agreement with the particle size data determined by PCS (Table 2).

3.6. Storage Stability Studies. The ability of the SLN to keep its physicochemical properties during storage was assessed at refrigerated conditions ($5 \pm 3^\circ\text{C}$) as well as at $25^\circ\text{C}/65\%$ RH for six months. After six-month storage at refrigerated conditions, there was insignificant difference in the PS for TP-SLN (F25) and TS-SLN (F26), while, in case of six-month storage at $25^\circ\text{C}/65\%$ RH, the particle size was increased significantly from the 123.1 ± 3.41 nm to 139.3 ± 3.82 nm for F25 and from the 132.6 ± 4.29 nm to 153.6 ± 4.74 nm for F26.

The EE (%) of the optimized batch TP-SLN (F25) and TS-SLN (F26) was initially found to be 86.6 ± 0.94 and 84.6 ± 0.81 , respectively, which was significantly decreased to 82.6 ± 0.29 and 79.3 ± 0.47 , respectively, after six-month storage at refrigerated conditions. The significant decrease in EE (%) was also observed when stored at $25^\circ\text{C}/65\%$ RH for 6 months and found to be 83.9 ± 0.14 and 78.6 ± 0.43 for TP-SLN (F25) and TS-SLN (F26), respectively, (Table 3).

The effect of pH on the stability of PZQ-loaded SLN was found to be remarkable (Table 3). The SLN kept in SGF (pH 1.2) for 2 hours showed increase in PS along with decrease in EE, whereas SLN kept for 6 hours in SIF (pH 6.8) were found to be stable. The results were in accordance with other published reports [19, 28].

Transitions of dispersed lipid from metastable forms to stable form might occur slowly on storage due to small particle size and the presence of emulsifier that may lead to drug expulsion from solid lipid nanoparticles [26, 28, 37]. The decreased EE observed on storage could be attributed to drug expulsion during lipid modification. An absolute large negative or positive ZP (130 mV) is required for stability of colloidal dispersion because the electrostatic repulsion could prevent the agglomeration. The ZP of the SLN was about -10 mV, which was not high enough to provide a strong electrical field around the particles, but measuring the PS of samples throughout storage period showed no significant changes in the PS of these samples. The stability studies confirmed that SLN stabilized with a combination of stabilizers (LG and

TABLE 3: (a) Particle size and entrapment efficiency of the PZQ-loaded SLN after storage at refrigerated temperature ($4 \pm 1^\circ\text{C}$) and at $25 \pm 1^\circ\text{C}/65 \pm 5\%$ RH (values are reported as mean \pm SD, $n = 4$). (b) Particle size and entrapment efficiency of the PZQ-loaded SLN after storage at different pH conditions (values are reported as mean \pm SD, $n = 4$).

(a)						
Formulations	Particle size (nm)			Entrapment efficiency (%)		
	Initially (0 hr)	After 6 months		Initially (0 hr)	After 6 months	
	RT	$4 \pm 1^\circ\text{C}$	$25 \pm 1^\circ\text{C}/65 \pm 5\%$ RH	RT	$4 \pm 1^\circ\text{C}$	$25 \pm 1^\circ\text{C}/65 \pm 5\%$ RH
TP-SLN (F25)	123.1 ± 3.41	128.1 ± 4.72	139.3 ± 3.82	86.6 ± 0.94	82.6 ± 0.29	83.9 ± 0.14
TS-SLN (F26)	132.6 ± 4.29	140.2 ± 5.11	153.6 ± 4.74	84.6 ± 0.81	79.3 ± 0.47	78.6 ± 0.43

(b)						
Formulations	Particle size (nm)			Entrapment efficiency (%)		
	Initially (0 hr)	pH 1.2 (2 hr)	pH 7.5 (6 hr)	Initially (0 hr)	pH 1.2 (2 hr)	pH 7.5 (6 hr)
	TP-SLN (F25)	123.1 ± 3.41	348.4 ± 6.93	169.2 ± 3.62	86.6 ± 0.94	34.4 ± 0.81
TS-SLN (F26)	132.6 ± 4.29	364.6 ± 7.46	184.6 ± 3.49	84.6 ± 0.81	36.1 ± 0.72	74.5 ± 0.95

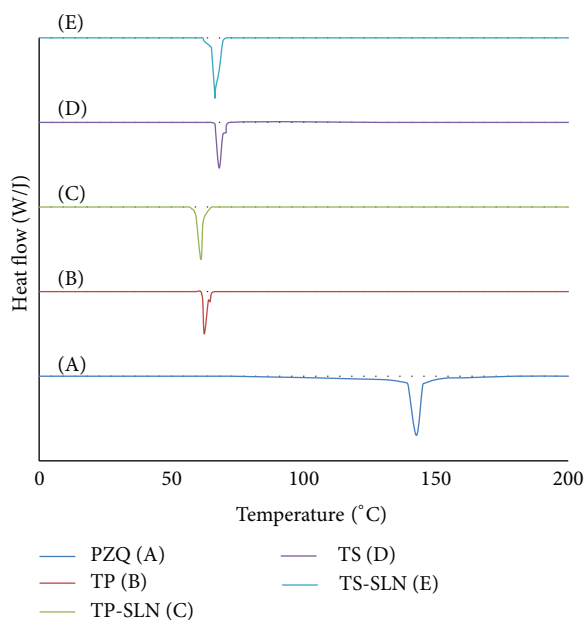


FIGURE 2: DSC thermograms of praziquantel (A), tripalmitin (B), praziquantel-loaded TP-SLN (C), tristearin (D), and praziquantel-loaded TS-SLN (E).

PI88) helped the SLN to remain stable over storage period. Storage at refrigerated conditions provided marginally better stability with regards to both PS and EE.

3.7. Differential Scanning Calorimetry Studies. DSC is a useful technique that gives an insight into the melting and recrystallization behavior of crystalline materials like SLN [43]. Figure 2 shows DSC thermograms of pure PZQ, tripalmitin, tristearin, and lyophilized PZQ-SLN. DSC thermogram of PZQ demonstrated that a sharp peak at 142°C corresponds to melting temperature of Praziquantel [44]. The thermograms of TP and TS bulk lipids showed endothermic peaks at 63.4°C and 69.6°C , respectively. In SLN formulations, the melting point of lipids were depressed in comparison to the melting

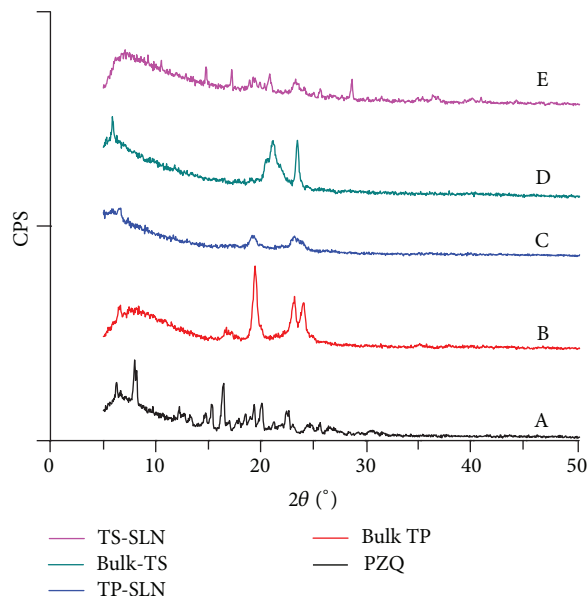


FIGURE 3: XRD patterns of praziquantel (A), tripalmitin (B), praziquantel-loaded TP-SLN (C), tristearin (D), and praziquantel-loaded TS-SLN (E).

point of the bulk lipid. This was attributed to the creation of lattice defects onto the lipid matrices following a decrease in their crystallinity in comparison to their bulk counterparts. The absence of PZQ melting peak in SLN indicates either formation of amorphous dispersion of PZQ in lipid matrix or solubilization of PZQ in lipid matrix upon heating.

3.8. X-Ray Diffractometry Studies. The XRD patterns of pure PZQ, tripalmitin, tristearin, and lyophilized PZQ-loaded SLN are shown in Figure 3. Powder XRD data confirmed the results obtained by DSC study. The diffraction pattern of PZQ indicates that drug is crystalline. The distinct sharp peaks were observed at 2θ scattered angles 6.2° and 7.9° and a series of peaks above 10° in the diffractogram. The XRD pattern corresponds to that of PZQ racemate crystal, as reported in

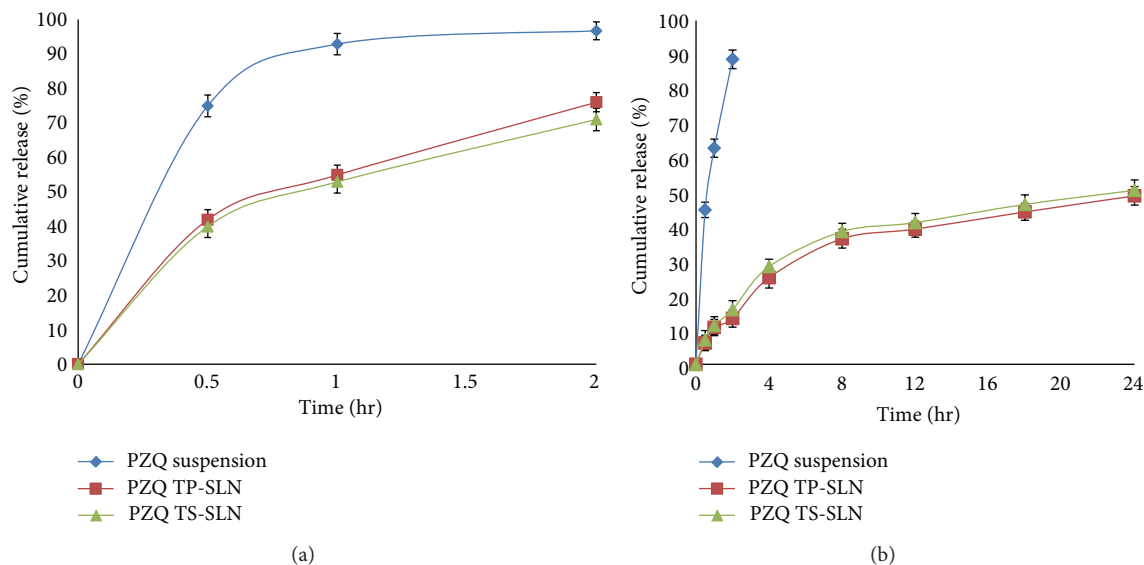


FIGURE 4: *In vitro* release profiles of PZQ-loaded SLN in (a) 0.1 N HCl (pH 1.2) and (b) phosphate buffer (pH 6.8).

TABLE 4: Pharmacokinetic parameters for praziquantel in rats after oral administration of PZQ-SLNs and PZQ suspension at an equivalent praziquantel dose of 50 mg/kg (values are means \pm SD, $n = 6$).

Formulation	T_{\max} (h)	C_{\max} ($\mu\text{g}/\text{mL}$)	$AUC_{0-\infty}$ ($\mu\text{g h}/\text{mL}$)	MRT (h)	$T_{1/2}$ (h)
PZQ suspension	0.17	2.16 ± 0.62	4.24 ± 1.156	2.67	1.86 ± 0.29
PZQ-SLN (F25)	0.33	1.81 ± 0.43	14.74 ± 2.36	14.18	11.49 ± 0.68

literatures [44]. However, these peaks could not be detected in diffractogram of PZQ-SLN which indicates that PZQ was solubilized within the lipid matrix of SLN and was in amorphous form in SLN. XRD pattern of TP showed sharp peaks at 2θ scattered angles around 5° and between 18 and 27° [28]; these characteristic peaks were observed in lyophilized PZQ-TP SLN indicating that TP remains in crystalline state. Similarly, TS (25.23°) was present in crystalline state in lyophilized SLN [28]. In addition, the XRD spectra obtained between angles $2\theta = 18$ and 25° , where the bulk lipids had sharp peaks, were lowered in the diffractograms of the SLN. This indicates that the less ordered crystal arrangements of the lipid matrix in the SLN formulations compared to the bulk solid lipid, such as amorphous state, would contribute to the higher drug loading capacity [43, 45].

3.9. *In Vitro* Drug Release Studies. The *in vitro* release pattern of PZQ-loaded SLN was determined in 0.1 N HCl (pH 1.2) for two hours and in phosphate buffer (pH 6.8) for 24 hours. During *in vitro* release studies, drug was released from the SLN and diffused through the dialysis membrane into the dissolution media, while the dialysis bag retained the SLN [32]. The results revealed that all the PZQ-loaded SLN formulations passing through the strong acidic environment of the stomach (as in 0.1 N HCl) tend to release a high amount of drug, whereas, in phosphate buffer (pH 6.8), the PZQ release from SLN was in a controlled manner (Figure 4). In phosphate buffer (pH 6.8), almost all the optimized SLN formulations showed initial burst release with the 25% of drug release within the first four hours followed by the sustained

release from the SLN. The slow release of the PZQ from all SLN formulations suggests homogeneous entrapment of the drug throughout the systems. Thus, the loading dose of the PZQ due to initial burst release can be obtained and followed by maintenance dose due to the sustained release by the PZQ-SLN which in turn will prevent the fluctuations in the PZQ plasma level. Similar sustained/prolonged drug release from the SLN was also observed by other researchers [19, 21, 28]. The PZQ release mechanism in phosphate buffer (pH 6.8) from the SLN formulation was analyzed by fitting the results using four kinetic models: zero order, which explains that the drug release rate as an independent phenomenon of the drug concentration; first order, which explains the drug release rate is proportional to its concentration; Higuchi, which is dependent on diffusion under Fick's law; and Korsmeyer-Peppas, when the drug release is a non-Fickian diffusion process. The determination coefficient (R^2) was used as an indicator of the best fitting of the data for each model. The release profiles of all the PZQ-SLN best fitted into the Higuchi equation ($R^2 = 0.986$) which describes the diffusion of drug from homogenous and granular matrix systems.

3.10. *Pharmacokinetic Study.* The plasma concentration-time profiles for the PZQ-SLN and PZQ suspension were shown in Figure 5. The pharmacokinetic parameters of PZQ were calculated using a noncompartmental analysis and were summarized in Table 4. The maximum plasma drug concentration (C_{\max}) after oral administration of PZQ-SLN was $1.8 \mu\text{g}/\text{mL}$ at 0.33 h and this was lower than that observed with the PZQ suspension ($2.16 \mu\text{g}/\text{mL}$ at 0.17 h). However,

TABLE 5: Pharmacokinetic parameters for praziquantel in rats after intraduodenal administration of PZQ-SLNs at an equivalent praziquantel dose of 50 mg/kg to rats treated with cycloheximide (CHM) and saline, respectively (values are means \pm SD, $n = 6$).

Formulation	T_{max} (h)	C_{max} ($\mu\text{g/mL}$)	$AUC_{0-\infty}$ ($\mu\text{g h/mL}$)	MRT (h)	$T_{1/2}$ (h)
PZQ-SLN + CHM	0.5	1.39 ± 0.15	3.37 ± 0.35	2.39	1.62 ± 0.36
PZQ-SLN + Saline	0.33	3.71 ± 0.19	19.58 ± 0.79	6.28	5.37 ± 0.95

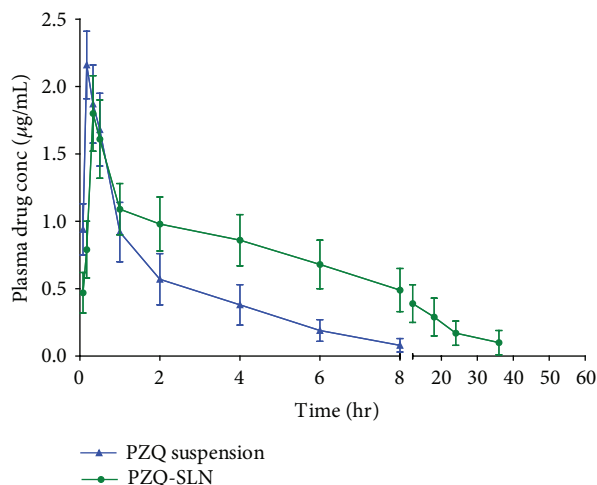


FIGURE 5: The mean plasma concentration-time curve after single oral administration of PZQ-SLN (F25) and PZQ suspension (0.5% w/v methyl cellulose suspension of pure PZQ) in rats (50 mg/kg) (values are means \pm SD, $n = 6$).

the decline in plasma concentration was slow and remained above the minimal effective concentration for 36 hrs [46]. The time to maximum drug concentration (T_{max}), half-life ($T_{1/2}$), and mean residence time (MRT) obtained with PZQ-SLN were significantly larger than those obtained with PZQ suspension. The MRT of PZQ-SLN is about five times greater than that with PZQ-suspension. The $AUC_{0 \rightarrow \infty}$ after oral administration of PZQ-SLN was 3.35-fold higher than that of PZQ suspension indicating the significant increase in bioavailability of PZQ ($P < 0.05$). The half-life of praziquantel increased from 1.86 hrs (PZQ suspension) to 11.5 hours (PZQ-SLN) when administered orally which reiterate the potential of SLN as a sustained release system. These results show that the incorporation of praziquantel into SLN leads to prolonged stay of PZQ in body; this could increase the duration of action of PZQ. The significantly enhanced oral absorption of SLN was consistent with that after the direct delivery to the intestine (intraduodenal administration), which indicated that the intestinal absorption was predominant in increasing the oral absorption of SLN (see Section 3.11).

3.11. Intestinal Transport of SLN. To investigate the transport of SLN after its uptake into the enterocytes, cycloheximide (CHM) was used to inhibit the lymphatic transport pathway without nonspecific damage to other active and passive absorption pathways [33–35]. The plasma concentration of PZQ in rats treated with CHM was significantly lower in comparison to rats treated with saline (Figure 6). When SLN

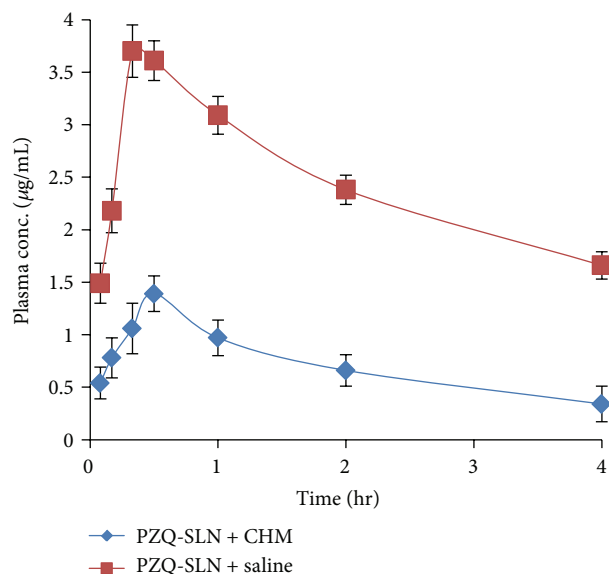


FIGURE 6: The mean plasma concentration-time curve after single intraduodenal administration of PZQ-SLN and PZQ suspension (0.5% w/v methyl cellulose suspension of pure PZQ) in rats (50 mg/kg) (values are means \pm SD, $n = 6$).

was intraduodenally administered to rats treated with CHM, the peak plasma concentration (C_{max}) of PZQ from SLN was significantly reduced by 62% and the $AUC_{0 \rightarrow \infty}$ of SLN decreased about 5.81-fold in comparison to values obtained with rats treated with saline (Table 5 and Figure 6). This could be attributed to CHM-induced blockage of intestinal lymphatic transport. The experimental results indicate that the intestinal lymphatic transport pathway plays a vital role in the intestinal transport of SLN into the systemic circulation.

4. Conclusion

In the present study, a poorly aqueous soluble drug PZQ was successfully incorporated into SLN by the hot homogenization followed by ultrasonication method. The type and ratio of the surfactants were important factors for the formulation. The results of the *in vitro* release experiments indicated a burst release at the initial stage and sustained release subsequently in simulated intestinal conditions. The rapid release of Praziquantel from SLN and increase in particle size in acidic environment indicate that there is a need to protect SLN from acidic environment of stomach to improve bioavailability via lymphatic transport. The lyophilized PZQ-SLN dispersions can be compressed into tablets which can be coated with suitable agent to avoid the effect of SGF.

Alternatively, either antacid, H₂-blockers, or proton pump inhibitors can be given before the administration of PZQ-SLN dispersion to avoid the effect of gastric pH on PZQ-SLN. An oral pharmacokinetic study in rats showed that SLN changed the pharmacokinetic parameters and resulted in significant improvement in the bioavailability of PZQ. SLN also extended the systemic circulation time of PZQ significantly. The PZQ-SLN could be a promising vehicle for delivery of PZQ for enhanced bioavailability along with reduction in dosing frequency and better patient compliance. However, it requires further *in vivo* evaluations on other diseased models for exploring therapeutic application of PZQ-SLN.

Conflict of Interests

The authors declare that there is no conflict of interests regarding the publication of this paper.

Acknowledgments

The first author is thankful to University Grant Commission (UGC), New Delhi, for the financial support in the form of Senior Research Fellowship (SRF). The authors are thankful to University Grants Commission, New Delhi, for providing financial assistance in the form of Major Research Project (F. no. 32-126/2006 (SR)). The authors are grateful to Professor G. Singh and Dr. Madhu Yashpal, Department of Anatomy, IMS-BHU, Varanasi, India, for carrying out the TEM analysis. The authors also acknowledge Special Assistance Programme (SAP) of UGC for providing instrumentation facility.

References

- [1] World Health Organization, *First WHO Report on Neglected Tropical Diseases*, 2012, <http://www.who.int/neglected-diseases/diseases/en/>.
- [2] J. Sotelo, O. H. del Brutto, P. Penagos et al., "Comparison of therapeutic regimen of anticysticercal drugs for parenchymal brain cysticercosis," *Journal of Neurology*, vol. 237, no. 2, pp. 69–72, 1990.
- [3] M. A. Urrea-París, M. J. Moreno, F. Rodriguez-Caabeiro, and N. Casado, "Chemoprophylactic praziquantel treatment in experimental hydatidosis," *Parasitology Research*, vol. 87, no. 6, pp. 510–512, 2001.
- [4] World Health Organization, *WHO Model List of Essential Medicines*, 17th edition, 2012, <http://www.who.int/medicines/publications/essentialmedicines/en/index.html>.
- [5] P. R. M. Bittencourt, C. M. Gracia, A. M. Gorz, and T. V. Oliveira, "High-dose praziquantel for neurocysticercosis: serum and CSF concentrations," *Acta Neurologica Scandinavica*, vol. 82, no. 1, pp. 28–33, 1990.
- [6] C. R. Caffrey, "Chemotherapy of schistosomiasis: present and future," *Current Opinion in Chemical Biology*, vol. 11, no. 4, pp. 433–439, 2007.
- [7] D. Cioli and L. Pica-Mattoccia, "Praziquantel," *Parasitology Research*, vol. 90, supplement 1, pp. S3–S9, 2003.
- [8] G. Leopold, W. Ungethuen, and E. Groll, "Clinical pharmacology in normal volunteers of praziquantel, a new drug against schistosomes and cestodes—an example of a complex study covering both tolerance and pharmacokinetics," *European Journal of Clinical Pharmacology*, vol. 14, no. 4, pp. 281–291, 1978.
- [9] H. Jung, R. Medina, N. Castro, T. Corona, and J. Sotelo, "Pharmacokinetic study of praziquantel administered alone and in combination with cimetidine in a single-day therapeutic regimen," *Antimicrobial Agents and Chemotherapy*, vol. 41, no. 6, pp. 1256–1259, 1997.
- [10] N. Castro, R. Medina, J. Sotelo, and H. Jung, "Bioavailability of praziquantel increases with concomitant administration of food," *Antimicrobial Agents and Chemotherapy*, vol. 44, no. 10, pp. 2903–2904, 2000.
- [11] S. K. El-Arini and H. Leuenberger, "Dissolution properties of praziquantel-PVP systems," *Pharmaceutica Acta Helveticae*, vol. 73, no. 2, pp. 89–94, 1998.
- [12] G. Becket, L. J. Schep, and M. Y. Tan, "Improvement of the *in vitro* dissolution of praziquantel by complexation with α -, β - and γ -cyclodextrins," *International Journal of Pharmaceutics*, vol. 179, no. 1, pp. 65–71, 1999.
- [13] M. Akbarieh, J. G. Besner, A. Galal, and R. Tawashi, "Liposomal delivery system for the targeting and controlled release of praziquantel," *Drug Development and Industrial Pharmacy*, vol. 18, no. 3, pp. 303–317, 1992.
- [14] S. C. Mourão, P. I. Costa, H. R. N. Salgado, and M. P. D. Gremião, "Improvement of antischistosomal activity of praziquantel by incorporation into phosphatidylcholine-containing liposomes," *International Journal of Pharmaceutics*, vol. 295, no. 1-2, pp. 157–162, 2005.
- [15] M. J. Doenhoff and L. Pica-Mattoccia, "Praziquantel for the treatment of schistosomiasis: its use for control in areas with endemic disease and prospects for drug resistance," *Expert Review of Anti-Infective Therapy*, vol. 4, no. 2, pp. 199–210, 2006.
- [16] L. Yang, Y. Geng, H. Li, Y. Zhang, J. You, and Y. Chang, "Enhancement of the oral bioavailability of praziquantel by incorporation into solid lipid nanoparticles," *Die Pharmazie*, vol. 64, no. 2, pp. 86–89, 2009.
- [17] S. Xie, B. Pan, M. Wang et al., "Formulation, characterization and pharmacokinetics of praziquantel-loaded hydrogenated castor oil solid lipid nanoparticles," *Nanomedicine*, vol. 5, no. 5, pp. 693–701, 2010.
- [18] M. K. Rawat, A. Jain, and S. Singh, "In vivo and cytotoxicity evaluation of repaglinide-loaded binary solid lipid nanoparticles after oral administration to rats," *Journal of Pharmaceutical Sciences*, vol. 100, no. 6, pp. 2406–2417, 2011.
- [19] R. Paliwal, S. Rai, B. Vaidya et al., "Effect of lipid core material on characteristics of solid lipid nanoparticles designed for oral lymphatic delivery," *Nanomedicine*, vol. 5, no. 2, pp. 184–191, 2009.
- [20] R. Holm and J. Hoest, "Successful *in silico* predicting of intestinal lymphatic transfer," *International Journal of Pharmaceutics*, vol. 272, no. 1-2, pp. 189–193, 2004.
- [21] S. S. Chalikwar, V. S. Belgamwar, V. R. Talele, S. J. Surana, and M. U. Patil, "Formulation and evaluation of Nimodipine-loaded solid lipid nanoparticles delivered via lymphatic transport system," *Colloids and Surfaces B*, vol. 97, pp. 109–116, 2012.
- [22] C. J. H. Porter and W. N. Charman, "Intestinal lymphatic drug transport: an update," *Advanced Drug Delivery Reviews*, vol. 50, no. 1-2, pp. 61–80, 2001.
- [23] C. J. H. Porter, N. L. Trevaskis, and W. N. Charman, "Lipids and lipid-based formulations: optimizing the oral delivery of lipophilic drugs," *Nature Reviews Drug Discovery*, vol. 6, no. 3, pp. 231–248, 2007.

- [24] A. Bargoni, R. Cavalli, O. Caputo, A. Fundarò, M. R. Gasco, and G. P. Zara, "Solid lipid nanoparticles in lymph and plasma after duodenal administration to rats," *Pharmaceutical Research*, vol. 15, no. 5, pp. 745–750, 1998.
- [25] R. H. Muller and C. M. Keck, "Challenges and solutions for the delivery of biotech drugs—a review of drug nanocrystal technology and lipid nanoparticles," *Journal of Biotechnology*, vol. 113, no. 1–3, pp. 151–170, 2004.
- [26] R. H. Müller, R. Shegokar, and C. M. Keck, "20 years of lipid nanoparticles (SLN & NLC): present state of development & industrial applications," *Current Drug Discovery Technologies*, vol. 8, no. 3, pp. 207–227, 2011.
- [27] M. R. A. Alex, A. J. Chacko, S. Jose, and E. B. Souto, "Lopinavir loaded solid lipid nanoparticles (SLN) for intestinal lymphatic targeting," *European Journal of Pharmaceutical Sciences*, vol. 42, no. 1–2, pp. 11–18, 2011.
- [28] V. Venkateswarlu and K. Manjunath, "Preparation, characterization and *in vitro* release kinetics of clozapine solid lipid nanoparticles," *Journal of Controlled Release*, vol. 95, no. 3, pp. 627–638, 2004.
- [29] W. Hanpitakpong, V. Banmairuroi, B. Kamanikom, A. Choe-mung, and K. Na-Bangchang, "A high-performance liquid chromatographic method for determination of praziquantel in plasma," *Journal of Pharmaceutical and Biomedical Analysis*, vol. 36, no. 4, pp. 871–876, 2004.
- [30] E. H. Gokce, G. Sandri, M. C. Bonferoni et al., "Cyclosporine A loaded SLN: evaluation of cellular uptake and corneal cytotoxicity," *International Journal of Pharmaceutics*, vol. 364, no. 1, pp. 76–86, 2008.
- [31] S. Das, W. K. Ng, P. Kanaujia, S. Kim, and R. B. H. Tan, "Formulation design, preparation and physicochemical characterizations of solid lipid nanoparticles containing a hydrophobic drug: effects of process variables," *Colloids and Surfaces B*, vol. 88, no. 1, pp. 483–489, 2011.
- [32] M. K. Rawat, A. Jain, A. Mishra, M. S. Muthu, and S. Singh, "Development of repaglinide loaded solid lipid nanocarrier: selection of fabrication method," *Current Drug Delivery*, vol. 7, no. 1, pp. 44–50, 2010.
- [33] A. Dahan and A. Hoffman, "Evaluation of a chylomicron flow blocking approach to investigate the intestinal lymphatic transport of lipophilic drugs," *European Journal of Pharmaceutical Sciences*, vol. 24, no. 4, pp. 381–388, 2005.
- [34] F. Gao, Z. Zhang, H. Bu et al., "Nanoemulsion improves the oral absorption of candesartan cilexetil in rats: performance and mechanism," *Journal of Controlled Release*, vol. 149, no. 2, pp. 168–174, 2011.
- [35] Z. Zhang, F. Gao, H. Bu, J. Xiao, and Y. Li, "Solid lipid nanoparticles loading candesartan cilexetil enhance oral bioavailability: *in vitro* characteristics and absorption mechanism in rats," *Nanomedicine*, vol. 8, no. 5, pp. 740–747, 2012.
- [36] S. Chakraborty, D. Shukla, B. Mishra, and S. Singh, "Lipid—an emerging platform for oral delivery of drugs with poor bioavailability," *European Journal of Pharmaceutics and Biopharmaceutics*, vol. 73, no. 1, pp. 1–15, 2009.
- [37] W. Mehnert and K. Mäder, "Solid lipid nanoparticles: production, characterization and applications," *Advanced Drug Delivery Reviews*, vol. 47, no. 2–3, pp. 165–196, 2001.
- [38] H. Bunjes, M. H. J. Koch, and K. Westesen, "Influence of emulsifiers on the crystallization of solid lipid nanoparticles," *Journal of Pharmaceutical Sciences*, vol. 92, no. 7, pp. 1509–1520, 2003.
- [39] F. D. Rumjanek and A. J. G. Simpson, "The incorporation and utilization of radiolabelled lipids by adult *Schistosoma mansoni in vitro*," *Molecular and Biochemical Parasitology*, vol. 1, no. 1, pp. 31–44, 1980.
- [40] E. K. Noriega-Peláez, N. Mendoza-Muñoz, A. Ganem-Quintanar, and D. Quintanar-Guerrero, "Optimization of the emulsification and solvent displacement method for the preparation of solid lipid nanoparticles," *Drug Development and Industrial Pharmacy*, vol. 37, no. 2, pp. 160–166, 2011.
- [41] H. Heiati, R. Tawashi, R. R. Shivers, and N. C. Phillips, "Solid lipid nanoparticles as drug carriers I. Incorporation and retention of the lipophilic prodrug 3'-azido-3'-deoxythymidine palmitate," *International Journal of Pharmaceutics*, vol. 146, no. 1, pp. 123–131, 1997.
- [42] M. A. Schubert, B. C. Schicke, and C. C. Müller-Goymann, "Thermal analysis of the crystallization and melting behavior of lipid matrices and lipid nanoparticles containing high amounts of lecithin," *International Journal of Pharmaceutics*, vol. 298, no. 1, pp. 242–254, 2005.
- [43] D. Hou, C. Xie, K. Huang, and C. Zhu, "The production and characteristics of solid lipid nanoparticles (SLN)," *Biomaterials*, vol. 24, no. 10, pp. 1781–1785, 2003.
- [44] Y. Liu, X. Wang, J. K. Wang, and C. B. Ching, "Structural characterization and enantioseparation of the chiral compound praziquantel," *Journal of Pharmaceutical Sciences*, vol. 93, no. 12, pp. 3039–3046, 2004.
- [45] P. Chattopadhyay, B. Y. Shekunov, D. Yim, D. Cipolla, B. Boyd, and S. Farr, "Production of solid lipid nanoparticle suspensions using supercritical fluid extraction of emulsions (SFEE) for pulmonary delivery using the AERx system," *Advanced Drug Delivery Reviews*, vol. 59, no. 6, pp. 444–453, 2007.
- [46] L. Pica-Mattoccia and D. Cioli, "Sex- and stage-related sensitivity of *Schistosoma mansoni* to *in vivo* and *in vitro* praziquantel treatment," *International Journal for Parasitology*, vol. 34, no. 4, pp. 527–533, 2004.



Hindawi

Submit your manuscripts at
<http://www.hindawi.com>

